GRIFFITH RELATION FOR SURFACE CRACKS PLACED IN BENDING

F. F. Lange
Material Sciences Department

Technical Report No. 7
N00014-68-C-0323

March 27, 1972

WESTINGHOUSE RESEARCH LABORATORIES
Beulah Road, Churchill Boro
Pittsburgh, Pennsylvania 15235

GRIFFITH RELATION FOR SURFACE CRACKS PLACED IN BENDING

F. F. LANGE

TECHNICAL REPORT NUMBER 7

OFFICE OF NAVAL RESEARCH
CONTRACT NO. N00014-68-C-0323

March 27, 1972

WESTINGHOUSE ELECTRIC CORPORATION
RESEARCH & DEVELOPMENT CENTER
MATERIAL SCIENCES DEPARTMENT
CHURCHILL BORO
PITTSBURGH, PENNSYLVANIA 15235

FOREWORD

This report was prepared at the Westinghouse Research and Development Center, Pittsburgh, Pennsylvania 15235. The work was sponsored by the Office of Naval Research under Contract Number N00014-68-C-0323.

GRIFFITH RELATION FOR SURFACE CRACKS PLACED IN BENDING

F. F. Lange

Westinghouse Research Laboratories
Pittsburgh, Pennsylvania 15235

ABSTRACT

The relation between flexural strength and crack size was investigated using glass specimens containing semi-elliptical shaped surface cracks with different lengths and depths. The value of the dimensionless factor in the Griffith fracture equation was found to vary between 2 to 3.8 depending on the crack depth to specimen thickness ratio. These results were compared to the theoretical results of others.

INTRODUCTION

Griffith[1] was the first to recognize the relation between strength and crack size. His thermodynamic treatment of this subject leads to the following relation:*

$$\sigma_c = A \left(\frac{\gamma E}{c}\right)^{1/2} \qquad (1)$$

where σ_c is the critical applied tensile stress that causes a crack of length c to propagate. The material properties E and γ are the Young's Modulus and fracture energy, respectively. A is a dimensionless factor.

An important scientific and engineering property of this expression is that, after rearrangement, it can be used as an analytical tool to estimate the size of the crack responsible for fracture:

$$c = A^2 \frac{\gamma E}{\sigma_c^2} \qquad (2)$$

To use this tool, knowledge of the material properties, viz. strength, elastic modulus, and fracture energy, and the factor A is required.

---

* This relation is for plane stress conditions. For plane strain conditions, a factor of $(1-\mu^2)^{-1/2}$ must be included, where μ = Poisson's Ratio.[2] When $\mu < 0.2$, this factor makes little difference in Eq. (1).

The factor A is the principal concern in this paper. Its value depends on several conditions, e.g., the mode of stressing, the ratio of specimen size to crack size and the type of crack under consideration.[3] Since flexural tests are commonly used to measure the strength of ceramics, it was the author's purpose to experimentally obtain the value of A for the case of a rectangular shaped specimen containing a surface crack placed in bending. Smith, et al.,[4] have published theoretical results concerning semi-circular surface cracks within a semi-infinite plate placed in pure bending. A correlation of the experimental data with these theoretical results will be made with respect to the relation between crack size and specimen dimensions.

EXPERIMENTAL

Glass microscope slides* (0.1 to 2.5 by 7.5 cm) were used as specimens for the following reasons:

(1) Both the fracture energy and the Young's Modulus have been reported for this glass.[5]

(2) Cracks can be slowly introduced into most glasses because they stress corrode easily.[6]

(3) Glass exhibits conchoidal fracture which helps to define the boundary of the crack by examining the fracture surface.

Surface cracks of the configuration shown in Fig. 1 were introduced into the center of each glass slide by first scribing with a diamond point. The scribed surface was then turned over onto a hollow cylinder. A crack was forced to propagate to the desired depth by pressing the surface opposite to the scribe mark with a blunt-pointed instrument. This was carried out under a binocular microscope, with oblique lighting. In most cases, the crack was extended beyond the scribe mark. Using this technique, cracks with lengths > 0.03 cm and depths > 0.005 cm could be formed easily. It should be noted that not

---

* Composition in weight percent: 72.8 SiO_2, 12.0 Na_2O, 8.8 CaO, 3.5 MgO, 0.9 Al_2O_3, 0.15 Fe_2O_3, 0.1 K_2O_3.

all scribe marks were satisfactory. Some formed many small cracks. Others, although observed plainly to be depressions by using the Nomarski interference contrast technique, would not form cracks. Such specimens were discarded.

Cracks with lengths < 0.02 cm could only be introduced by indenting the surface with a diamond point. For these, the crack lengths and depths could not be controlled as they were for the larger cracks.

Flexural strength measurements were performed using a four-point loading device (shown in Fig. 2) that used tool steel rods (0.30 cm diameter) contained in "v" grooves to load the specimen. The distance between inner and outer loading positions were 1.90 and 3.80 cm, respectively. A crosshead speed of 0.05 cm/min was used.

All strength measurements were conducted in a liquid nitrogen ambient to minimize crack extension prior to catastrophic fracture due to stress corrosion.[6] It was found that crack extension during the cooling from room temperature to 77°K could be avoided by quickly immersing the whole specimen into the liquid nitrogen.

The strength was calculated with the following equation:

$$\text{Strength} = \sigma = \frac{Mt}{2I} \qquad (3)$$

where M = bending moment, t = specimen thickness, and I = moment of inertia of the rectangular cross section.

The crack lengths and depths were measured after fracture using a microscope-cathetometer with an accuracy of ± 0.0001 cm. When the proper oblique lighting was used, the initial crack boundaries

could be clearly observed on the fracture surface as a ridge which was caused by the slight change in the fracture plane when the crack was extended during fracture (see Fig. 3). For crack lengths < 0.03 cm, this technique could not be used due to the uneven fracture surface topography adjacent to the crack. Therefore, the crack lengths were measured prior to fracture with the microscope-cathetometer using oblique lighting to illuminate the crack. Depth measurements could not be made for these smaller cracks.

STRENGTH RESULTS

Table I lists the strength, the crack length, the crack depth, and the ratio of crack depth to crack length for each fractured specimen. The specimens are listed in the order of the strongest to the weakest. All cracks were semi-elliptical in shape.

All but 5 of the specimens contained cracks that were small relative to the specimen's width, i.e., $c/w < 0.1$. Most of the crack depths were comparable to the specimen's thickness, i.e., $0.06 < d/t < 0.6$.

With a few exceptions, the decrease in strength corresponded to an increase in crack length. Because the cracks were semi-elliptical in shape (for most, $0.15 < d/c < 0.30$), their depths were dependent on their lengths; thus, in most cases, the strength decreased with increasing crack depth. However, when the strength of specimens with similar crack lengths but different crack depths were analyzed, it was found that the strength did not vary by more than ± 8% for a 100% change in crack depth. This analysis suggested that the crack length had a greater influence on strength than the crack depth. The influence of crack depth will be discussed in a latter section.

FRACTURE SURFACE TOPOGRAPH

Several different topographical features on the fracture surfaces indicated the mode of crack propagation. Besides the ridge that marked the initial crack boundary, much smaller ridges outlined the shape of the moving crack front. Hackle and crack branching were also observed.

The smaller ridges were the only topographical features observed on specimens containing large cracks. Figure 4a schematically illustrates the pattern of these ridges which were difficult to photograph. This pattern shows that the major axis of this semi-elliptical shaped crack front increased at a greater rate than its minor axis indicating that it had a greater velocity along the tensile surface than through the specimen thickness. Hackle developed on the fracture surface of specimens that contained smaller cracks (illustrated in Fig. 4b). The pattern of ridges indicated that the hackle hindered the crack front movement. Crack branching (shown in Fig. 4c) occurred for the smallest cracks. From these observations, it was apparent that the amount of stored strain energy prior to fracture (which is determined by the stress at fracture) governed the crack velocity, which in turn governed the amount of hackle and crack branching that occurred.*

* Yoffee has shown that crack branching depends on crack velocity.(7)

DETERMINATION OF A

By rearranging Eq. (1), a value of the numerical factor A was calculated for each specimen:

$$A = \frac{\sigma (c)^{1/2}}{(\gamma E)^{1/2}} \qquad (4)$$

The material properties $\gamma = 4.52 \times 10^3$ ergs/cm^2 and $E = 7.34 \times 10^{11}$ dyn/cm^2 have been reported previously by Widerhorn[5] for the glass slide composition used in the present work. Examining the results of these calculations reported in Table I, one can see that A lies between 2-4 and, in general, A increases with decreasing strength. These results will be analyzed with respect to theoretical results obtained by Smith, et al.[4]

The stress intensity factor, K_I, has been calculated by Smith, et al., for a semi-circular shaped surface crack within a semi-infinite plate placed in pure bending. The crack that they considered was small relative to the plate's width, but comparable in size to the plate's thickness (t), i.e., $c/w \ll 1$, and $c/t = 0$ to 1. Except for the crack shape, these conditions are similar to the experimental cracks investigated in the present work. Their calculations resulted in the following expression:

$$K_I = F \left(\frac{2\sigma\sqrt{c}}{\sqrt{2\pi}}\right) \qquad (5)$$

where σ is the maximum tensile stress on the surface of the plate (as determined in Eq. (3)), and F is a numerical factor with a value between 0.3 and 1.2 depending on the position along the crack front and the crack depth to plate thickness ratio (d/t). For a given d/t, F was largest where the crack front intercepted the surface, and smallest at the crack's greatest depth, i.e., K_I is largest at the surface. Hence, Smith, et al., showed that the semi-circular crack would grow into a semi-elliptical shaped crack before catastrophic fracture would occur. For such an equilibrium shaped, semi-elliptical crack, the value of K_I would be the same for all positions along the crack front. This condition implies that the factor F in Eq. (5) depends only on the d/t ratio. Thus, for an equilibrium shaped, semi-elliptical crack, K_I depends only on the d/t ratio and the length of the crack (c) as measured on the surface.

The relation between K_I and the material properties γ and E is[8]

$$K_I = \sqrt{2\gamma E} \, . \tag{6}$$

By combining Eqs. (1), (5) and (6) a relation between A and F is obtained:

$$A = \frac{\sqrt{\pi}}{F} \tag{7}$$

Since F depends only on the crack depth to specimen thickness ratio (d/t) this relation suggests that the experimental values of A should depend on the d/t ratio. Figure 5 illustrates the values of A for $c/w < 0.1$

plotted against d/t. The solid curve in this figure illustrates the theoretical values of A derived from Eq. (7) using the minimum values of F reported by Smith, et al. Although the experimental values of A show much scatter, they also increase as d/t increases similar to that of the theoretical curve. Thus, it was concluded that the numerical factor A in Griffith's equation depends on the crack depth to specimen thickness ratio. The scatter in the experimental values of A is most likely due to both the errors in crack size measurements and the fact that most cracks were not of an equilibrium shape.

The results of Smith, et al., show that the equilibrium shape of the semi-elliptical crack depends on the d/t ratio. As d/t increases, the c/d ratio also increases. Examination of Table I shows that this relation was not followed for the cracked glass plates.

DISCUSSION

This work has shown that values of A lie between 1.8 and 3.5 depending on the crack depth to specimen thickness ratio (d/t). When $d/t \to 0$, which may be the condition most expected for very small cracks in large flexural ceramic bar specimens, A is equal to either $\sqrt{\pi}$ based on the theoretical results of Smith, et al., or ~ 2 based on the experimental results obtained in the present work. The value of A chosen for determining the crack size responsible for fracture is important since it is a squared factor (see Eq. (2)). Many investigators, including this author, have used values of A not applicable to flexural strength measurements which have resulted in crack size estimates 2-4 times too small. This is particularly important when crack size estimates are related to microstructure, e.g., grain size, to explain the strength behavior of polycrystalline ceramics.

Another important implication of this work is that a similar surface crack in two different specimens sizes can result in a significantly different strength. This can be seen by examining the effect of the d/t ratio on A (Fig. 5). For fixed crack dimensions, A is larger for a specimen where $d/t \to 0.5$, relative to a thick specimen where $d/t \to 0$, i.e., very thin specimens are expected to have a higher flexural strength than thick specimens.

The effect of specimen thickness on strength was examined for hot-pressed silicon nitride fabricated for another investigation. Two sets of bar specimens (approximate dimensions: thick bars: 0.32 x 0.63 x 3.2 cm; thin bars: 0.07 x 0.32 x 3.2 cm) were diamond cut from the same hot-pressed disc. Both sets were placed in 4 point flexural loading (distance between inner points = 0.635 cm, outer points = 1.875 cm). The thick bars had in a flexural strength of 75,000 ± 2% psi, whereas the thin bars had a strength of 97,000 ± 15% psi. The crack size was estimated to be 140 μm based on γ = 39,000 ergs/cm (fracture energy measurements were made on the same hot-pressed disc), E = 44.5 x 10^6 psi, σ = 75,000 psi and $A = \sqrt{\pi}$. The higher strength of the thin bars is likely due to a larger value of A relative to the thick bars. The decreased volume under stress can also cause the thin specimens to exhibit a higher strength. Thus, the crack size to specimen thickness ratio must be considered when designing flexural strength experiments.

ACKNOWLEDGMENTS

The author would like to thank J. J. Nalevanko for his technical help.

TABLE I

STRENGTH, CRACK DIMENSIONS, AND THE NUMERICAL FACTOR A FOR GLASS SPECIMENS

Strenth, psi x 10^3	Crack length (c), cm	Crack Depth (d), cm	d/c	A
19.7	0.011	—	—	2.47
19.2	0.010	—	—	2.30
18.1	0.013	—	—	2.47
15.7	0.012	—	—	2.06
14.3	0.020	—	—	2.42
12.3	0.030	0.006	0.20	2.55
12.2	0.029	0.006	0.21	2.48
11.6	0.034	—	—	2.56
9.85	0.054	0.015	0.22	2.74
9.77	0.044	0.009	0.20	2.45
9.47	0.041	0.012	0.29	2.29
9.06	0.063	0.006	0.10	2.72
8.99	0.078	0.020	0.25	3.00
8.93	0.051	0.008	0.16	2.41
8.89	0.078	0.024	0.31	2.97
8.52	0.065	0.012	0.18	2.60
8.33	0.078	0.022	0.30	2.78
8.23	0.073	0.014	0.19	2.66
8.16	0.076	0.009	0.12	2.69
7.60	0.075	0.024	0.32	2.49
7.26	0.108	—	—	2.84
6.95	0.165	0.039	0.21	3.38
6.72	0.155	0.029	0.19	3.17
6.71	0.171	0.011	0.06	3.32
6.65	0.160	0.022	0.14	3.18
6.37	0.176	0.028	0.16	3.20
6.31	0.197	0.034	0.17	3.35
6.19	0.173	0.032	0.18	3.08
6.16	0.203	0.028	0.13	3.37
5.57	0.246	0.046	0.19	3.31
5.23	0.254	0.058	0.22	3.15
5.08	0.324	0.053	0.16	3.46
5.03	0.258	0.052	0.20	3.06
4.93	0.310	0.057	0.18	3.29
4.79	0.411	0.058	0.14	3.68
3.85	0.690	0.074	0.11	3.83
3.26	0.960	0.070	0.07	3.82

REFERENCES

1. A. A. Griffith, "The Phenomena of Rupture and Flow in Solids", Phil. Trans. Roy. Soc. Lon. 221A [4], 163-198 (1920).
2. R. A. Sack, "Extension of Griffith's Theory of Rupture to Three Dimensions", Proc. Phys. Soc. Lon. 58, 739-736 (1946).
3. W. F. Brown, Jr. and J. E. Srawley, Plane Strain Crack Toughness Testing of High Strength Metallic Materials, ASTM Special Publication, No. 410, (1966).
4. F. W. Smith, A. F. Emergy and A. S. Kobayashi, "Stress Intensity Factors for Semi-Circular Cracks, Part 2 — Semi-Infinite Solid", Trans. ASME, J. Appl. Mech. Paper No. 67-WA/A PM-2 (1967).
5. S. M. Wiederhorn, "Fracture Surface Energy of Glass", J. Am. Ceram. Soc. 52 [2], 99-105 (1969).
6. S. M. Wiederhorn, "Fracture Surface Energy of Soda-Lime Glass", Materials Science Research Vol. 3, Ed. by W. W. Kriegel and H. Palmore III, Plenum Press, New York, 503-528 (1966).
7. E. H. Yoffee, "The Moving Griffith Crack", Phil. Mag. 42 [2], 739-750 (1951).
8. G. R. Irwin, Handbuck der Physik, Vol. 6, Springer, Berlin, (1958).

Dwg. 2960A30

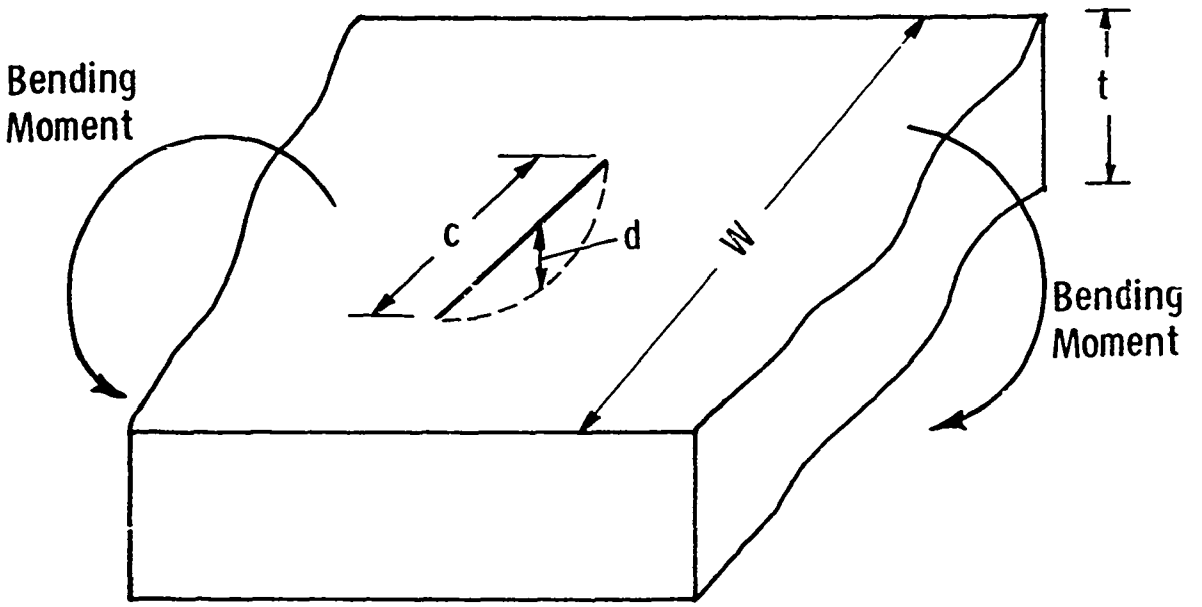

Figure 1—Illustration of the type of surface crack investigated

Dwg. 2960A28

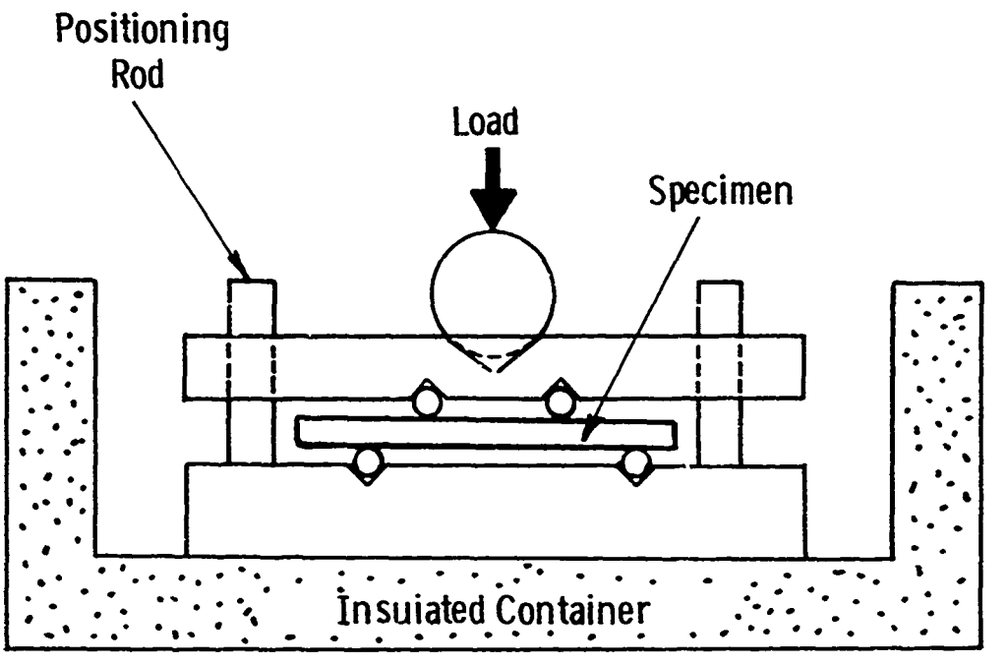

Figure 2—The four point loading device

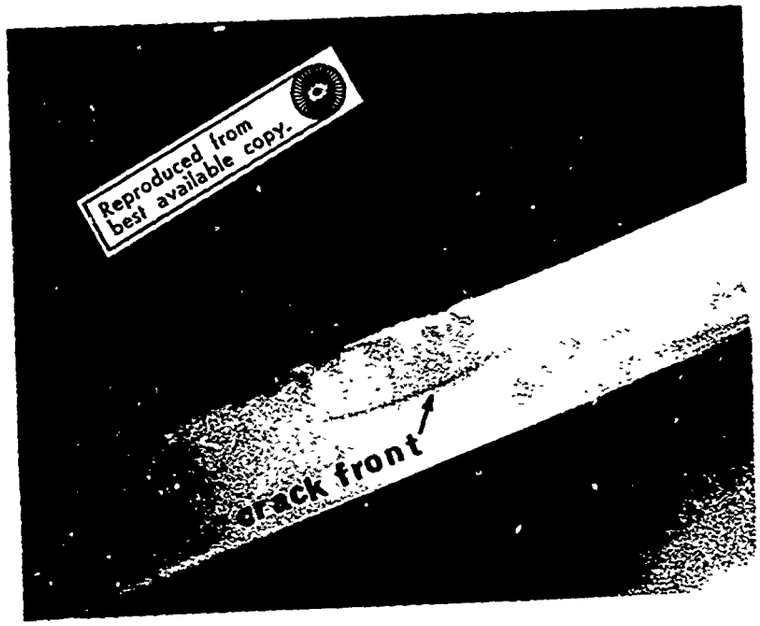

FIGURE 3 - Fracture surface showing ridge that marks the crack front prior to crack propagation

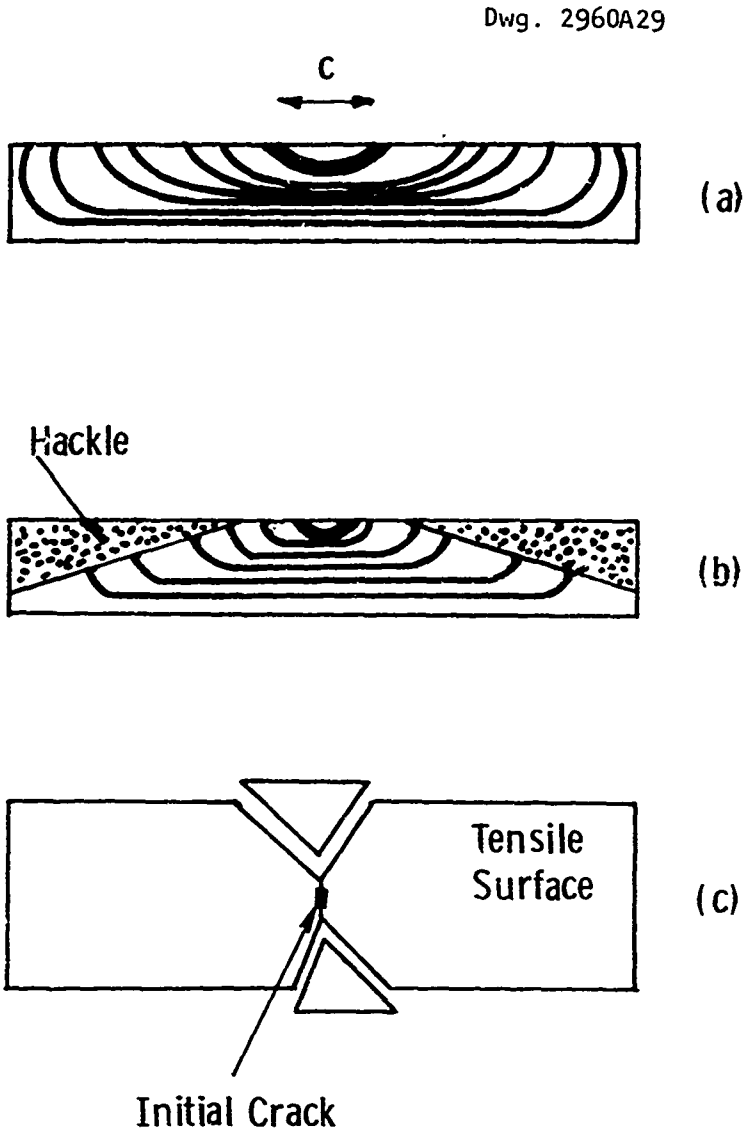

Figure 4—Three different modes of crack propagation

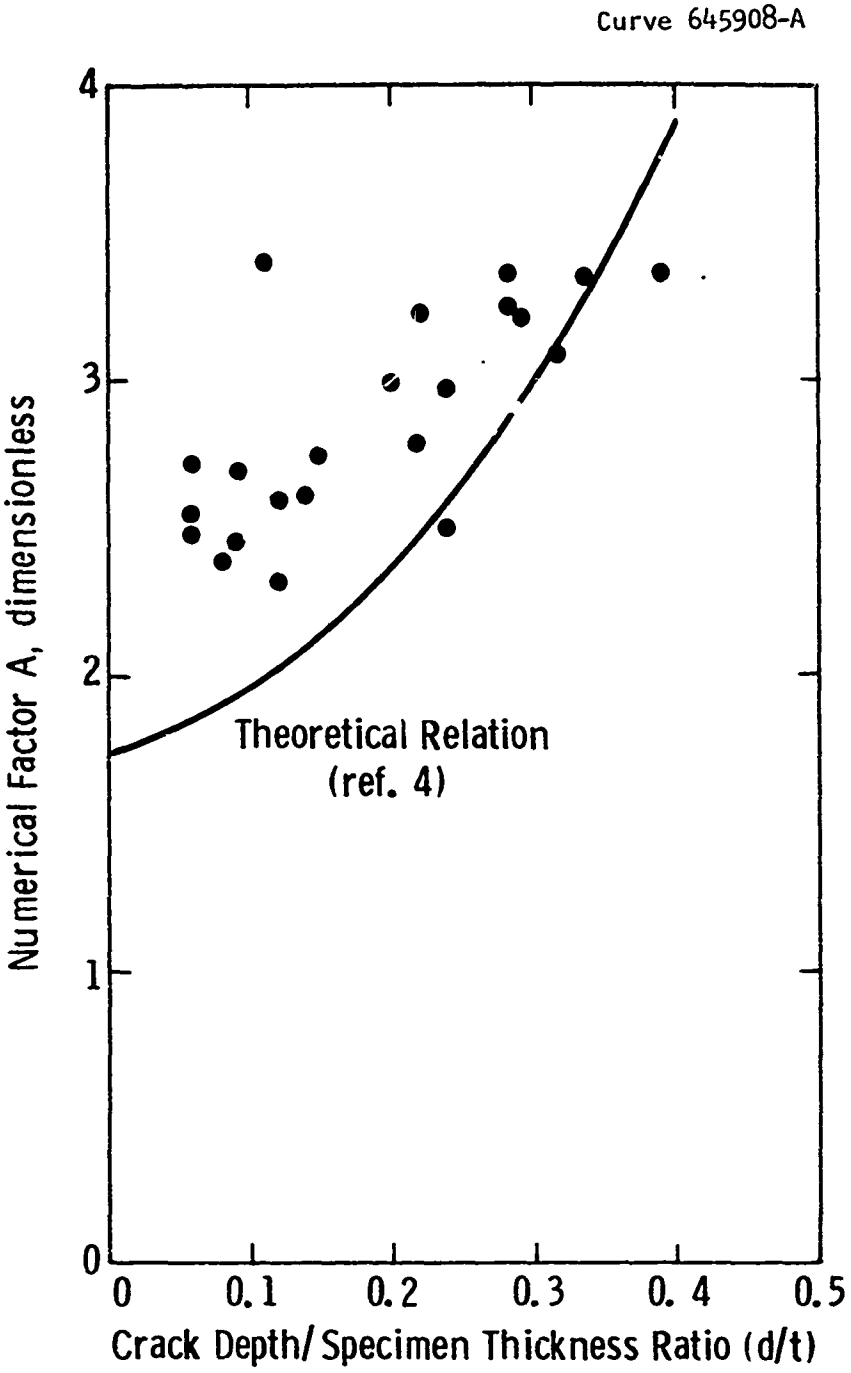

Figure 5—Numerical factor A vs crack depth/specimen thickness ratio. Points are experimental results and solid line is theoretical relation of Smith et al.[4]